Modeling Urban Population Growth from Remotely Sensed Imagery and TIGER GIS Road Data

Fang Qiu, Kevin L. Woller, and Ronald Briggs

Abstract

We modeled population growth from 1990 to 2000 in the north Dallas-Fort Worth Metroplex using two different methods: a conventional model based on remote sensing land-use change detection, and a newly devised approach using GIS-derived road development measurements. These methods were applied at both city and census-tract levels and were evaluated against the actual population growth. It was found that accurate population growth estimates are achieved by both methods. At the census-tract level, our models yielded a comparable result with that obtained from a more complex commercial demographics model. At both city and census-tract levels, models using road development were better than those using land-use change detection. In addition to being efficient in cost and time, our models provide direct visualization of the distribution of the actual population growth within cities and census tracts when compared to commercial demographic models.

Introduction

The scale and rapidity of recent urban growth in large metropolitan areas is without precedence (Weeks *et al.*, 2000; Yang, 2002). As a result, increased research interest is being directed to the mapping and monitoring of urban sprawl using GIS and remote sensing techniques (Epstein *et al.*, 2002). Accelerating urban growth is usually associated with, and driven by, the population concentration in the area. However, the measurement and estimation of population using newer, more accurate, and more detailed data is not well studied to date (Longley and Mesev, 2002). Accurate and current population information is of great interest in growing urban and suburban areas for such diverse purposes as urban planning, resource management, marketing analysis, service allocation, etc. Unfortunately, the conventional census of population is extremely expensive and thus is only conducted in most countries once every decade. Consequently, no accurate population information is available for any year between two consecutive decennial censuses (Lo, 1995).

For this reason, demographic models have been employed in order to predict intercensal population based on previous census figures combined with a variety of other data, such as local economic indicators, counts obtained from consumer marketing databases, postal service delivery statistics, etc. (Claritas, unpublished material, 2002). These methods may provide reasonable predictions, but the implementation of these models is often complex and expensive due to the requirement for collecting multiple inputs and the involvement of significant manpower for demographic analysis. The success of these models relies heavily on the prediction performance in the previous year and on other current local estimates, whose accuracy can never be verified. Additionally, demographic models often generalize over an administrative unit (e.g., a city or a county) and fail to pinpoint the exact location within the unit where the population growth occurred.

Remotely sensed images provide alternative opportunities for estimating population in urban and suburban areas. Large-scale aerial photographs have long been used to count the number of dwelling units observed from the air and to estimate total population based on average household size for each dwelling type (Noin, 1970; Watkins and Morrow-Jones, 1985; Lo, 1986). This method works well for small areas but, when used to model the population of an entire metropolitan region, it requires a large number of aerial photographs and is very time-consuming. Satellite imagery, such as SPOT, Landsat MSS and TM data, as well as DMSP nighttime data, have also been employed to measure population size and population density (Lo, 1995; Sutton, 1997; Weeks *et al.*, 2000; Dobson *et al.*, 2000; Lo, 2001). Because of its synoptic view and multispectral characteristics, satellite imagery allows measurements related to population and the identification of its spatial concentration within larger administrative units in an efficient manner.

The purpose of this paper is to estimate the population growth from 1990 to 2000 in the northern Dallas-Fort Worth Metroplex, an area of known high population growth in the past decade. Two different methods are employed. The first uses a traditional model based on land-use change detected from remote sensing data. The second approach is based on measures of new road development derived from GIS data. To the best of our knowledge, the latter approach to population estimation had not been reported in the literature when the initial work on this research was completed (Woller, 2001; Qiu *et al.*, 2002), although a recent study employed road networks for mapping suburban sprawl (Epstein *et al.*, 2002). The effectiveness and efficiency of these two different methods were examined at both the city and census-tract levels using the actual population data from the Census Bureau as a reference. The estimation results of these two methods were also compared

F. Qiu and R. Briggs are with the Program in Geographic Information Sciences, School of Social Sciences, University of Texas at Dallas, Richardson, TX 75083-0688 (ffqiu@utdallas.edu; briggs@utdallas.edu).

K.L. Woller is with Pioneer Natural Resources USA, Inc., 5205 N. O'Connor Blvd., Suite 1400, Irving, TX 75039-3746 (wollerk@pioneernrc.com).

Photogrammetric Engineering & Remote Sensing
Vol. 69, No. 9, September 2003, pp. 1031–1042.

0099-1112/03/6909–1031$3.00/0

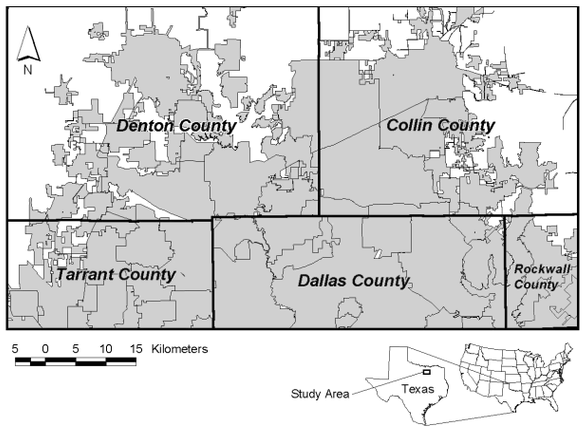

Figure 1. Study area in the north Dallas-Fort Worth Metropolitan region.

with those obtained from a commercial demographic model at the census-tract level. The benefits and the costs of these two methods were then evaluated and summarized in terms of prediction accuracy and processing difficulty.

Study Area

The study area is located in the northern Dallas-Fort Worth Metroplex as shown in Figure 1, covering nearly 5000 square kilometers (1930 square miles) of total area. The study area comprises all of Collin, Denton, and Rockwall counties and northern parts of Dallas and Tarrant counties in north Texas. Some of these counties are among the fastest growth areas of the United States in the past decade. For example, Collin County grew 86 percent in population from 1990 to 2000, ranking 11th out of 3,141 U.S. counties. Denton County grew 58 percent and ranked 53rd in the nation. Urban sprawl in the past decade is mainly clustered in the north part of the metropolitan area due to the concentration of high-tech telecommunication industries. In the heart of this area is the complex of major multinational technology corporations known as the Telecom Corridor. Built-out areas in central and south Dallas and Tarrant counties show very little population growth in the last ten years and were not included in the study area.

Data

Remote Sensing Data

The remote sensing data used in this study are comprised of two Landsat images acquired on the same day-of-the-year, i.e., 19 August 1991 and 19 August 2000 (Figure 2). Using anniversary-date imagery removes seasonal sun angle and minimizes phenological differences that may be harmful to a change-detection study (Jensen, 1996). Ideally, the remote sensing image for the preferred census year of 1990 should be employed. It was not used because, unfortunately, the scene was covered with too many clouds. Multitemporal remote sensing images are commonly used in change-detection studies, but their use in estimating population growth has not been widely reported. The 1991 image was acquired by Landsat 5's Thematic Mapper (TM) sensor and covers Path 027, Row 037 of the Landsat Worldwide Reference System. The 2000 image was acquired by Landsat 7's Enhanced Thematic Mapper Plus (ETM+) sensor and covers the same path and row as the 1991 image. The thermal bands of the two images and the panchromatic band of the ETM+ were not included in the analysis because of their incompatible spatial resolution. The spatial resolution of all other bands is 28.5 meters. The color composites of bands 4, 3, and 2 (near-infrared, red, and green) for the two images are displayed in Figure 2.

The urban growth in the study area is apparent even through simple visual comparison of the two images. The general growth trend is from south to north in the study area. This is evidenced on the remotely sensed data by the many new clearings of land (appearing as white in the year 2000 image) in the north, while almost no change of land-use type is found in the south.

TIGER Road Data

The U.S. Census Bureau's TIGER (Topologically Integrated Geographic Encoding and Referencing) road data were used for measuring the length of new road development from 1990 to 2000. Although TIGER files are not the most accurate transportation data set, it is the best available that is frequently updated at known dates. There are more accurate transportation data sets, especially for the year 2000, but without documented dates, it is impossible to calculate the road change over time. The 1990 and 2000 TIGER files were obtained from U.S. Census Bureau data CDs published in 1992 and from the ESRI website (www.esri.com/data/download/census2000_tigerline/index.html, last accessed 07 June 2003), respectively. The necessary GIS operations were performed to transform the raw data into ArcView shapefiles and to project the shapefiles into the desired projection (UTM, Zone 14 N). The projected shapefiles were then clipped to the geographical extent of the study area.

An overlay comparison of the roads for the two study years reveals considerable growth in both the number and the length of roads in the study area (Figure 3). Green lines represent all existing roads in 1990 and the red lines show new roads constructed thereafter and until 2000. The new road development occurs primarily in the northern fringes of the study area (Figure 3a). A zoomed view of the map (Figure 3b) demonstrates the road development between the two years in more detail. The layout of these new roads indicates that most new road construction was related to housing expansion, and others were associated with commercial developments in the study area.

Population Data

The U.S. Census Bureau was the ultimate source of the population data used in the study. However, the actual digital data came from several different sources. The 1990 population data were extracted from CDs issued by the U.S. Census Bureau. The 2000 tabular population data came from North Texas Council of Governments (NTCOG). The 1990 and 2000 census-tract and census-block boundaries were downloaded from the ESRI Geography Network website. The data for the counties under study was identified and extracted. The tabular data and census-tract polygon data were then joined using a unique ID.

The targets of interest of our study are population changes at the city and census-tract levels. However, census-tract boundaries do not exactly match between 1990 and 2000. In addition, some of the census tracts are not completely contained within one city, but cross two or more city boundaries. Therefore, in order to ensure maximum accuracy, we aggregated the block-level population data for each city and each census tract using year 2000 boundaries. The generated population counts at the city level for the year 2000 were checked against the actual census values and were found to be identical.

Population growth was obtained by subtracting the population of 1990 from that of 2000 at the city and census-tract level. The growth areas (not shown) corresponded to the known areas of expansion in the northern Dallas-Fort Worth Metroplex,

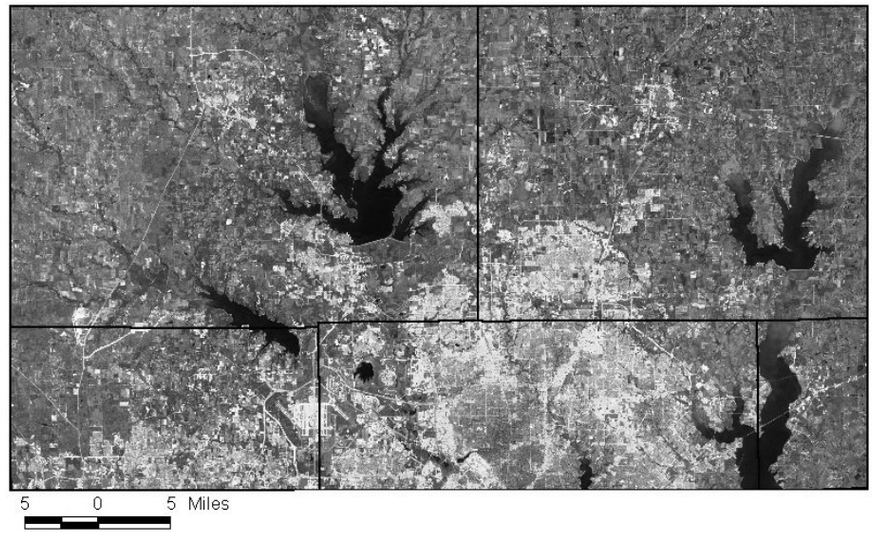

(a)

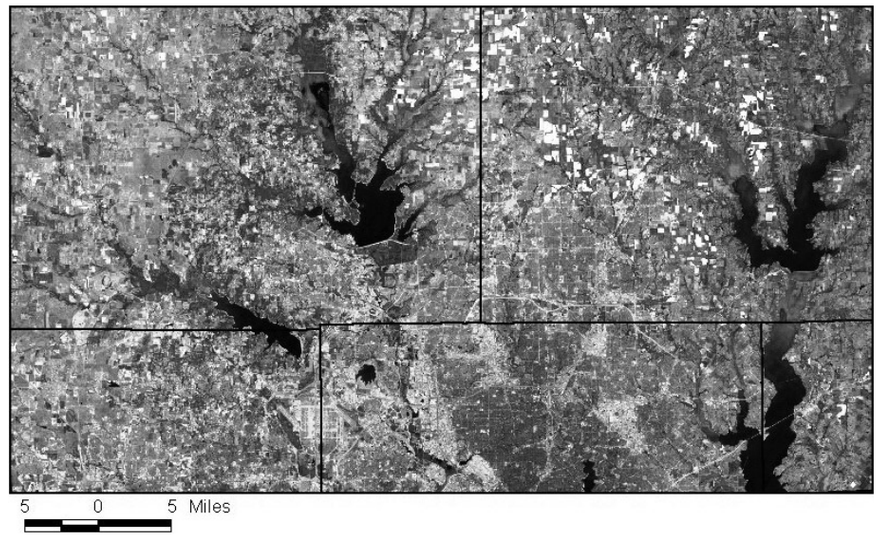

(b)

Figure 2. Remote sensing images of the study area for 1991 and 2000. (a) Landsat TM image for 1991. (b) Landsat ETM+ image for 2000. (Color version at ASPRS website: www.asprs.org.)

particularly the cities of Flower Mound, Lewisville, Carrollton, Plano, and Frisco. They also generally agreed with the areas with substantial new urban growth and road development observed on the remote sensing images and TIGER road files.

Research Methodology

The estimation of population growth at the city and census-tract levels was accomplished by using two different techniques. The first technique was a traditional remote sensing digital land-use change-detection approach using 1991 TM and 2000 ETM+ images, while the second technique was a GIS-based "new road development" measurement approach using 1990 and 2000 TIGER road data. For short, we call them the remote sensing (RS) and GIS models, respectively, which were then statistically correlated with and regressed against population growth measures derived from the 1990 and 2000 population data from the U.S. Census Bureau. The estimates obtained from the two population growth models were then compared with the actual population data and with the predictions from a commercial demographic model (Claritas, unpublished material, 2002) at the census-tract level.

Image Processing and Change Detection

Jensen (1996) recommends a series of digital image processing steps for a land-use change analysis using remotely sensed data. For our study, the following steps were identified as appropriate: geometric registration, radiometric normalization, image classification and sorting, and the application of a change-detection algorithm.

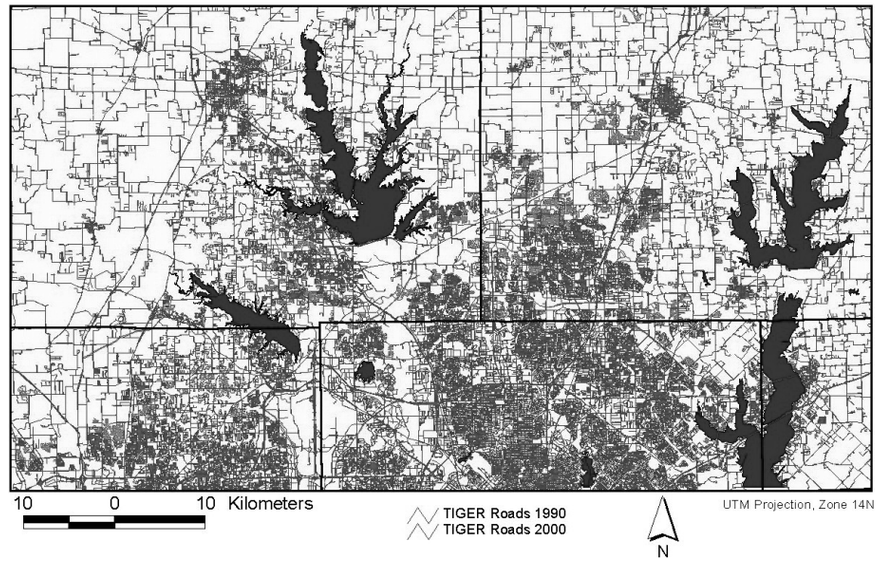

(a)

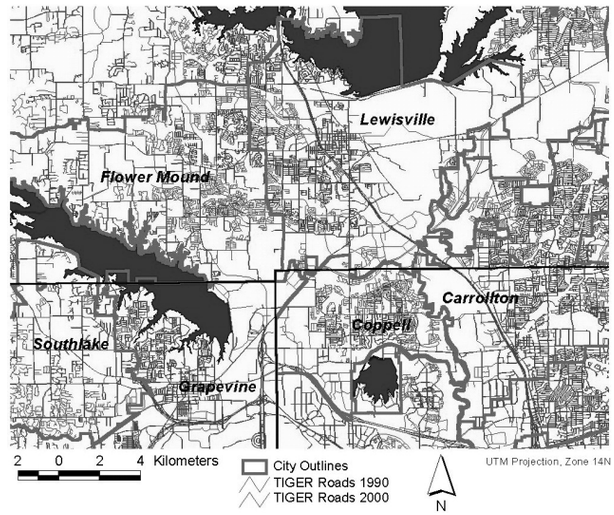

(b)

Figure 3. Overlaid TIGER road maps for 1990 and 2000. (a) Overview. (b) Zoomed view. (Color version at ASPRS website: www.asprs.org.)

Although the remotely sensed data acquired were claimed to be georectified, the accuracy of the rectification was not satisfactory for change detection purposes. Additional geometric rectification was performed using a first-order polynomial transformation and nearest-neighbor resampling to accurately match the images to the best available precision road data (not the TIGER data). The resultant root-mean-square error of less than 0.5 pixel values was obtained for both 1991 and 2000 images.

Multiple-date empirical radiometric normalization on the remote sensing data was then performed to correct the radiometric difference caused by sun angle, atmospheric, and soil moisture condition changes. The empirical radiometric normalization method was chosen over the absolute radiometric correction method because no atmospheric and soil moisture conditions were available for the time the images were acquired. Radiometric control targets that do not significantly change spectrally from time to time, such as water, roads, airport runways, parking lots, and building roofs, were used to normalize the 1991 image to the 2000 image. A regression equation was estimated by correlating the brightness of the control targets present in both the 1991 and 2000 images.

Jensen (1996) summarizes the various algorithms for digital change detection, and many examples of applied change-detection analysis are reviewed by Lunetta and Elvidge (1998). Other analyses of change in urban land use are examined by Zhan *et al.* (1998). For this study, the post-classification comparison change-detection approach was selected because it provides both the quantitative measure of land-use change and the "from-to" change-class information. However, this

approach requires an accurate classification on both the "from" and the "to" images. To this end, a classification scheme has to be established before the image classification operation. We adopted a modified Anderson Level I Land Use/Land Cover Classification System (USGS, 1992), which included urban/built-up land, water, agriculture land, rangeland, forestland, and barren land. Given this study's focus on urban change detection, the differentiation of agriculture land, rangeland, forestland, and barren land is unnecessary. Consequently, these classes were grouped into a composite class referred to as vegetated/barren land. As a result, a simplified classification scheme containing three classes, namely, urban, water, and vegetated/barren land, was actually used to document land-use change.

The unsupervised ISODATA (Interactive Self-Organizing Data Analysis) technique (Jensen, 1996) proved to be the most efficient and accurate approach to identifying spectral clusters of the two images in this study. It was performed with the following parameters: 20 classes, ten maximum iterations, 0.95 convergence threshold, skip factors of 1,1 (all data used). Following the unsupervised clustering, each of the 20 spectral classes were assigned to an appropriate information class and then grouped into one of the three main land-use classes, i.e., urban, water, and vegetated/barren land.

A close examination of the resultant classification images revealed the existence of spontaneous classification errors in the form of salt-and-pepper patterns at the class boundaries and within classes. These spontaneous errors were usually small in area and result from the mixed pixel and anomalous noise problems common to Landsat data (Yang, 2002). To deal with these errors, a focal majority filtering is usually applied to the classified image. However, the size of the moving window for the filter has to be very large for the noise to be sufficiently removed, which raises the possibility of altering between-class edges, resulting in blocky polygons with zigzagged boundaries (Jensen *et al.*, 2001). We explored an adaptive region-filtering technique to reduce the spontaneous classification errors (Ormsby and Alvi, 1999, pp. 305–310). This was carried out by creating regions (contiguous cells) for each land-use type on the classified images. All regions less than or equal to 5 pixels are identified and labeled as masks. Then a nibble operator is applied to fill in the masked pixels with the information class of its nearest neighbors. With this post-classification sorting approach, the spontaneous errors were substantially removed and the between-class boundaries were also well preserved. On-site verification of classified images using GPS and comparisons with large-scale aerial photographs were conducted. The overall, user's, and producer's classification accuracies for both images were all above 90 percent (Table 1). Therefore, the image classifications were of sufficient quality for further change-detection analysis.

To quantify the change in land use from 1991 to 2000, a post-classification comparison change-detection algorithm was developed using image algebra. The original classification images have values of 1, 2, 3 assigned to the water, vegetated/barren land, and urban classes, respectively. We multiplied the 1991 classification image by 10 and added the result to the 2000 image. The new values in the resultant image thus contain the information for both unchanged land-use types and the "from-to" change types. Table 2 shows the code schemes for the output change-detection image, where the diagonal elements stand for unchanged land-uses and off-diagonal elements for "from-to" changes. For example, value 11 represents the unchanged water class, whereas value 23 indicates land-use change from vegetated/barren land to urban. Table 2 also provides the color scheme used to display the change detection image. Pixels that stay the same retain their original red, blue, or green color for urban, water, or vegetation, respectively, while other colors were assigned to the change types.

TABLE 1. REMOTE SENSING IMAGE CLASSIFICATION ACCURACY ASSESSMENT

Classification Data	Reference			Row Total	User's Accuracy
	Water	Vegetation	Urban		
A. Classification Agreement Table for the 1991 Image					
Water	49	1	0	50	98.0%
Vegetation	0	45	5	50	90.0%
Urban	0	2	48	50	96.0%
Column Total	49	48	53	150	100%
Producer's Accuracy	100.0%	93.8%	90.6%	100%	94.7%*
B. Classification Agreement Table for the 2000 Image					
Water	49	1	0	50	98.0%
Vegetation	0	45	5	50	90.0%
Urban	0	3	47	50	94.0%
Column Total	49	49	52	150	100%
Producer's Accuracy	100.0%	91.8%	90.4%	100%	94.0%†

*Overall classification accuracy = 94.7%
†Overall classification accuracy = 94.0%

TABLE 2. CHANGE-DETECTION CODE AND COLOR MATRIX

	2000					
	Water		Vegetated/Barren		Urban	
1991	Code	Color	Code	Color	Code	Color
Water	11	Blue	12	Dark Green	13	Pink
Vegetated/Barren	21	Medium Blue	22	Bright Green	23	Magenta
Urban	31	Light Blue	32	Medium Green	33	Red

Our interest is focused on the changes from other land-use types to the urban type. Here, magenta is used for changes from vegetated/barren land to urban, and pink for change from water to urban.

To provide indices of urban growth, we simply sum the number of pixels for the urban land-use category in the 1991 and 2000 images for each research unit and then calculate the difference by simple subtraction. These are input into the population growth models discussed below.

Measuring New Road Development with GIS

Compared with the remote sensing change detection approach, the process used to measure road length is very simple and is based on one of the most commonly used GIS overlay operations. The "intersect" operation was selected to overlay the TIGER road files with the city or census-tract polygon files, because city and census are our basic research units. The "intersect" operation computes the geometric intersection of the two layers involved. Only those roads in the area common to both layers are retained in the output. The road segments are preserved if they fall within the boundaries of a city or a census-tract polygon, and are clipped when they intersect with the boundaries of a polygon. The output from the "intersect" operation is a split road system with an attribute table containing items from the original road segment and the identification number (ID) of the polygon within which the road is now contained. After computing the length for each clipped road segment, a summary statistic for polygons was obtained by summing the length of the roads completely within each polygon. New road development was then derived as the difference in the total road length for each city/census-tract polygon between the years 1990 and 2000.

Population Growth Modeling

Previous studies on population estimation using single-date satellite remote sensing data either made use of the extent of residential or urban area measured from the image, or directly correlated the pixel brightness values of various bands with population counts (Lo, 2001). In this study, however, multitemporal remote sensing images are involved and the target of interest is population growth. Although pixel brightness values have been used in spectral change-vector analysis to detect land-use change (Malila, 1980; Michalak, 1993), a direct link of spectral change vectors with population growth is difficult to establish. Consequently, only the change in the area of urban land-use was employed in our first model of population growth. A linear regression model in the following form was established to estimate population growth:

$$PG = a + b^*A_c \quad (1)$$

where PG is population growth, A_c is area change in urban land-use (as a pixel count), a is the regression intercept, and b is the slope. Both a and b have to be empirically determined using a subset of the samples.

The second model used is based on the correlation between GIS-derived new road development and population growth. The linear regression model thus established is

$$PG = a + b^*L_r \quad (2)$$

where PG is population growth and L_r is the road development in kilometers. Again, the parameters a and b are regression intercept and slope, respectively, which need to be determined empirically.

The remote sensing and GIS models were each applied to the data set at both the city and census tract level. At the city level, a total of 59 cities and towns within the study area were used. Five "central cities" (Dallas, Addison, Highland Park, University Park, and Fort Worth) in central and south Dallas and Tarrant counties were not included in the study area. However, many of the cities that could arguably be considered as a stable urbanized area with fringes of growth (such as Richardson) were included in order to ensure a sufficient sample size and to test the robustness of our population estimation models. The cities were stratified into quartiles based on population growth during the study period. A selection set of 29 cities was assembled by randomly selecting seven cities within each quartile plus one more randomly selected from the entire group. These 29 selected cities were used to estimate the linear regression models, while the remaining 30 cities were used to assess the validity of the models.

At the census-tract level, a total of 143 tracts were identified to match the areas used by a commercial demographic model (Claritas, unpublished material, 2002), which also encompassed the geographic scope of the city-level analysis. Because the commercial demographic model was not available at the city level, a fair comparison of its population estimates with our models was only possible at the census-tract level. Again, these 143 census tracts were stratified into quintiles according to the population change from 1990 to 2000, six tracts were randomly selected within each quintile to form a subset of 30 tracts, and the linear regression model was derived. The remaining 113 census tracts were reserved for validating the accuracy of the regression models.

To evaluate the predictive power of the population growth models, an array of error measures were computed based on the difference between the predicted and the actual population growth (i.e., the prediction error at each research unit) using the validating data set. For comparison purposes, the same statistics were also generated for the output from the commercial demographic model applied at the census-tract level. These measures included the three common population error statistics used by Lo (1995; 2001), namely, total % error, mean relative % error, and mean absolute % error.

Total % error is calculated as the ratio of the total prediction error (i.e., the sum of all prediction errors for all units) over the total population in 2000. The total % error is a good global indicator of how good the model is for estimating the overall population in the whole study area. However, people often care more about the performance of the models at each local research unit (i.e., a city or a census tract). This is especially true for those who work for the cities and communities, such as city managers and urban planners. Unfortunately, total % error is not necessarily a good local measure of predictive power since a perfect total % error (a measure of zero) can result from large overestimations and underestimations in each individual research unit that cancel each other. Mean relative % error is obtained by first calculating local % error for each unit (i.e., the ratio of prediction error over the population count at the unit) and then averaging the local % errors for all of the research units. Mean relative % error is a better error measure at the local level, but again negative and positive local % errors can cancel each other. Mean absolute % error, derived by averaging the absolute values of the local % errors in the study area, avoids the cancellation problem. However, this measure is usually heavily affected by the extremes. The same prediction error can have an extremely high absolute local % error in a research unit with a very small population base, but can also have an extremely low absolute local % error in a research unit with a large population base. Therefore, the mean absolute % error is still not an ideal measure of prediction errors.

To deal with this problem, we introduce two more error measures: the median absolute % error, and the population weighted average absolute % error. The median absolute % error is the 50th percentile of local absolute % errors. Like the mean, the median is also a measure of central tendency, but it is not affected by outliers. The population weighted average absolute % error is defined as the ratio of the population weighted sum of local absolute % errors over the sum of all the populations. The use of population as a weight normalizes local absolute % error and makes it possible to eliminates the extreme effects on the measure caused by the difference in population base. We believed the population weighted average % error is the best local error measure. With the use of this error measure, research units with small populations would cease to pull the measure toward a higher value, and units with large populations would not push the measure in the lower value direction.

The estimated population growth was also used to compute the predicted total population in 2000 for each city and census tract in the validation data set. This was compared with the actual population in 2000 from the U.S. Census to further evaluate the accuracy of the predictive models.

Results and Discussion

The remote sensing image classifications for the two study years are shown in Figures 4a and 4b, respectively. A comparison of the two images reveals substantial changes in urban land use from 1991 to 2000, indicating a rapid urban expansion in the area during the past 9 to 10 years. Another visible change is the shrinkage of the water class, especially obvious at Grapevine Lake and Lake Lewisville, the two big lakes in the western half of the study area. This shrinkage was due to the significant difference in moisture between the two study years. Weather station rainfall data indicate that 2000 was an extremely dry year.

The change-detection image obtained from these two classified images according to the coding and coloring schemes

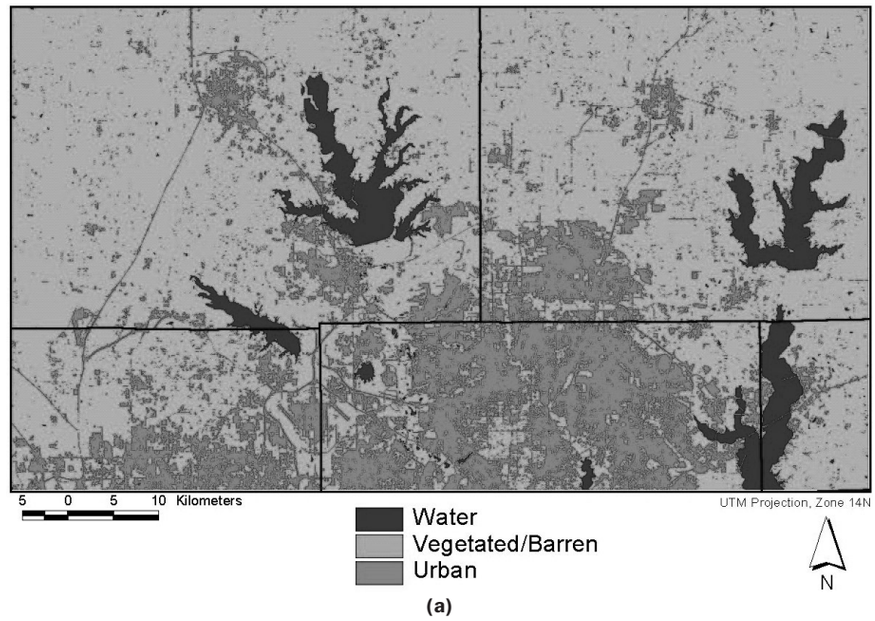

Figure 4. Remote sensing classification results. (a) Classified image for 1991. (b) Classified image for 2000. (Color version at ASPRS website: www.asprs.org.)

defined in Table 2 is shown in Figure 5. Table 3 summarizes the number of pixels of each change type and its associated percentage in the change-detection image. The change from vegetated/barren land to urban (in magenta) is the most prevalent change type, with a total area of about 603 square kilometers, or 12.1 percent of the study area. The change from water to vegetated/barren land (in dark green) is primarily visible only in the upstream part of lakes in the west (0.7 percent). The amount of change from water to urban is relatively small (0.2 percent). These are unlikely real changes, and are probably related to the drier conditions and the lower lake levels in 2000. There is very little change (0.1 percent) from vegetated/barren land to water and literally no change from urban to water. The areas that appear to have undergone a change from urban to vegetation are largely the results of misclassification found mainly in the central urban areas that were excluded from our study area, where the tree canopy extended during the ten-year period and covered the concrete or asphalt formerly exposed to aerial view in 1991. This misclassification was also the reason that built-out areas in central and south Dallas and Tarrant counties were excluded from the study area.

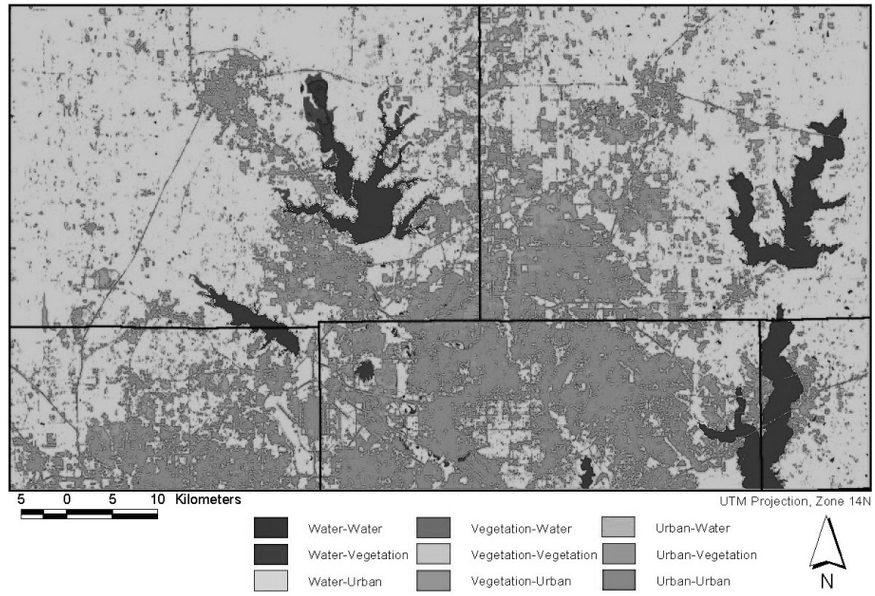

Figure 5. Land-use change detection map. (Color version at ASPRS website: www.asprs.org.)

The urban land-use change in pixels and the new road development in kilometers derived above were used as the independent variables in the remote sensing and GIS models, respectively, to estimate population growth. The Pearson correlation coefficients (r) between urban land-use change and population growth, and between road development and population growth (Table 4), were first calculated using all the sample data at the city ($n = 59$) and the census-tract ($n = 143$) levels. Table 4 clearly revealed that urban land-use change and road development are strongly and significantly correlated with population growth. At both city and census-tract levels, the correlations between road development and population growth were found to be almost perfect and much stronger than those between urban land-use change and population growth. Generally, the correlation coefficients at the city level were higher than those at the census-tract level.

The 29 cities that were selected out of the 59 samples using the quartile stratified randomization method were then used to calibrate the linear regression models for the urban change and road development data. The two models obtained are as follows:

$$PG = 1410.824 + 1.017{*}A_c \ (with\ r^2 = 0.61, P < 0.0001) \quad (3)$$

and

$$PG = -1859.14 + 200.437{*}L_r \ (with\ r^2 = 0.95, P < 0.0001) \quad (4)$$

where PG, A_c, and L_r are population growth, urban land-use change in pixel count, and new road development in kilometers, respectively. The slope coefficient in regression Equation 3 indicates that an increase of 1 pixel (28.5 by 28.5 meters) of urban area would be associated with an addition of approximate one person, while the slope in regression Equation 4 reveals that every kilometer of new road development would be accompanied by an addition of approximately 200 people to the population in the cities. The r^2 of the two models suggested that the GIS-based model yielded an almost perfect goodness-of-fit to the selected data, and was much better than that of the remote-sensing-based model.

These two models were then applied to the 30 cities that were withheld to assess prediction accuracy. The resulting

TABLE 3. CHANGE-DETECTION MATRIX

	2000							
	Water		Veg./Barren		Urban		1991 Totals	
1991	km²	%	km²	%	km²	%	km²	%
Water	254	5.1	37	0.7	11	0.2	302	6.1
Veg./Barren	4	0.1	3066	61.7	603	12.1	3673	73.9
Urban	1	0.0	154	3.1	842	16.9	997	20.1
2000 Totals	259	5.2	3256	65.5	1456	29.3	4972	100

TABLE 4. PEARSON'S CORRELATION COEFFICIENTS (r) BETWEEN THE NEW URBAN AND ROAD DEVELOPMENT AND THE POPULATION GROWTH AT THE CITY AND CENSUS-TRACT LEVELS

Levels	Correlation Variables	Urban Change Vs. Population Growth	New Road Develop Vs. Population Growth
City Level	($n = 59$)	0.83*	0.96*
Census-Tract Level	($n = 143$)	0.79*	0.93*

*Highly significant

TABLE 5. ERROR MEASURES FOR THE POPULATION GROWTH MODELS AT THE CITY LEVEL

	Total % Error	Mean Rel. % Error	Mean Abs. % Error	Median Abs. % Error	Population Weighted Average Abs. % Error
RS Model	1.1	−136.1	140.4	41.9	13.8
GIS Model	−2.7	79.9	113.1	21.3	13.6

TABLE 6. CENSUS-TRACT LEVEL POPULATION ESTIMATION ERRORS FOR THE GIS-BASED AND RS-BASED MODELS COMPARED WITH THOSE OF THE COMMERCIAL DEMOGRAPHIC MODEL

	Total % Error	Mean Rel. % Error	Mean Abs. % Error	Median Abs. % Error	Population Weighted Average Abs. % Error
RS Model	3.0	−11.1	22	12.5	20
GIS Model	3.7	−8.1	17	10.5	14
Commercial Model	−1.1	−3.6	21	16.1	19

estimates of the population growth were compared with the actual counts, and the various error measures described previously were derived. The results are reported in Table 5. The RS-based model produced a very small total % error (1.1 percent), indicating its power for predicting overall population. It was even better than the GIS-based model (−2.7 percent), which seems to contradict our earlier observations. However, a close examination of all other local error measures shows that the GIS-based model is consistently superior to the RS-based model. Deemed as the best local indicator of prediction accuracy, the population weighted average % error reveals that both models achieve an accuracy of about 87 percent at the city level, with the GIS model being slightly better.

Similarly, at the census-tract level, the 30 tracts generated by the quintile stratified randomization approach were used to calibrate the RS and GIS regression models as follows:

$$PG = 805.204 + 0.978^{*}A_c \ (with\ r^2 = 0.63, P < 0.0001) \quad (5)$$

and

$$PG = 543.89 + 177.341^{*}L_r \ (with\ r^2 = 0.84, P < 0.0001) \quad (6)$$

with PG, A_c, and L_r as defined before. The results are consistent with those found at the city level. For example, the RS-based regression model (Equation 5) predicts approximately one person ($b = 0.978$) per pixel of urban area, which is same as that of the RS model at the city level. The GIS-based regression model (Equation 6) produced a rate of 177 people per kilometer of new road development, comparable with that at the city level of 200 people/kilometer. The r^2 of the two models is also similar to that at the city level. Although the goodness of fit for the GIS-based model at the census-tract level is less (0.84 compared to 0.95), it was still much better than that of the RS-based model (0.63).

The GIS- and RS-based regression models were also applied to the remaining 113 census tracts for validation purposes. Additionally, at the census-tract level, it was possible to include comparisons with predictions from the commercial demographic model. The various error measures are displayed in Table 6. The commercial demographic model achieved the best total % error (−1.1 percent), and the RS-based model (3.0 percent) is slightly better than the GIS-based model (3.7 percent) in terms of estimating overall population growth. However, the conclusions drawn from the global accuracy indicator could not be extended to those from the local accuracy indicators. For example, the GIS-based model is always better than the RS-based model for all four local error measures. The commercial demographic model yielded the lowest accuracy in terms of the median absolute % error (16 percent), which may indicate that large overestimates and underestimates exist for the model. Based on the population weighted average absolute % error, the GIS-based model was the most accurate estimator (14 percent) and was much better than the other two models. The measures for the RS-based model (20 percent) and the commercial demographic model (19 percent) are comparable to each other. Compared to the accuracies of the models at the city level, the GIS-based model at the census level was about the same, while the RS-based model exhibited a decline from 86 percent to 80 percent in accuracy.

The estimated population growths obtained from these models were then employed to predict the 2000 population data. The results at both the city and census-tract level are displayed in Figures 6 and 7, respectively, in the form of cross-plots. Linear regressions between the predicted and the true population were also conducted for further accuracy assessment. A perfect population prediction is expected to yield a slope of 1 and an intercept of 0 in the regression function. The deviation from the expected values and goodness of fit (r^2) of the regression function are alternative ways to measure prediction errors. At the city level (Figure 6), the GIS-based model has a slope closer to 1 (1.0347), a better goodness of fit (0.9914), but a slightly larger intercept (−1101.9) than the RS model (with a slope, intercept, and r^2 of 0.9284, 763.53, and 0.8649, respectively). Based on all three of the above measures at the census-tract level (Figure 7), the GIS model was consistently the best model, while the RS model was also consistently better than the demographic model. The associated scatter plots also supported this observation: the scatter points of the GIS model are more concentrated along the regression line. However, the commercial demographic model tended to underestimate small populations, while the RS model was likely to underestimate large populations.

Overall, compared to the commercial demographic model, the RS- and GIS-based models produced either superior or at least equivalent results at the census-tract level. In addition, the by-products of these models offer the possibility of mapping where the estimated population growth is likely to be distributed spatially in each census tract or city, an option not provided by the commercial demographic model. Figures 8a and 8b show zoomed views of the change in urban land use and the new road development from 1990 to 2000 derived in the RS- and GIS-based models, respectively. These two maps provide the information about where the majority of the population growth is expected to occur, although a small amount of population increase in the established urban area is also possible. The comparison of these two maps reveals general agreement, with the exception that changes to urban land use tend to extend beyond the geographic scope established by the road development, especially in the northern part of the region shown. Further investigation found that these extended areas are primarily either new residential areas under construction without inhabitants as yet or other non-residential urban land use. This may help explain why the RS model was less accurate than the GIS model, because the latter is based on the established road network in communities already populated.

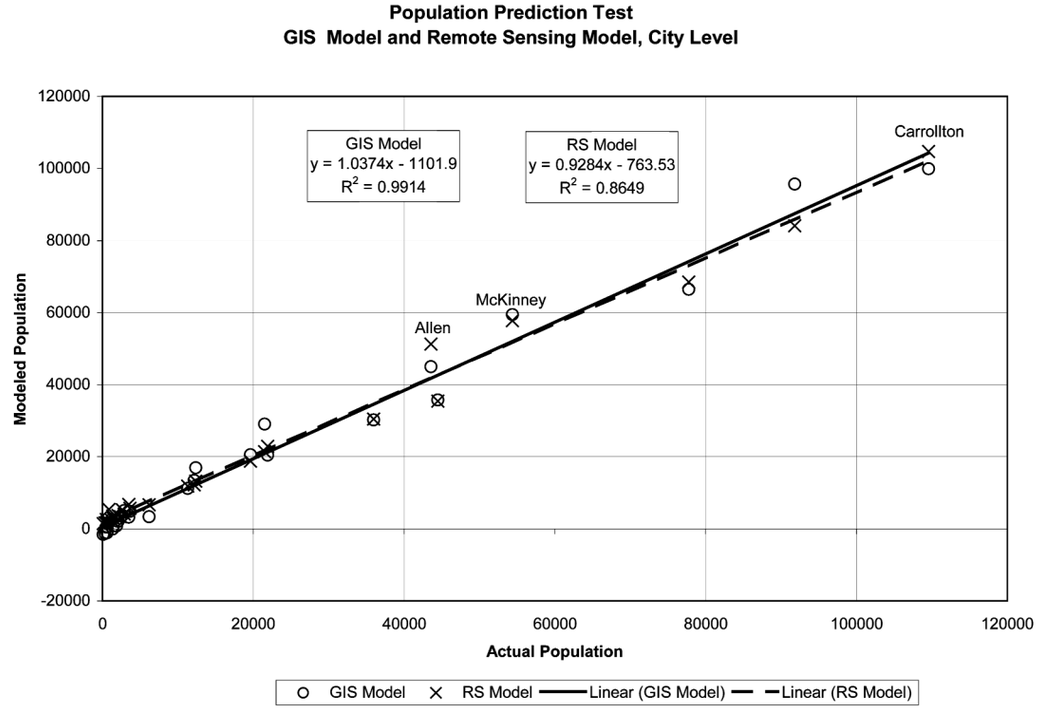

Figure 6. Cross plot of predicted population by different models and actual population in 2000 at the city level.

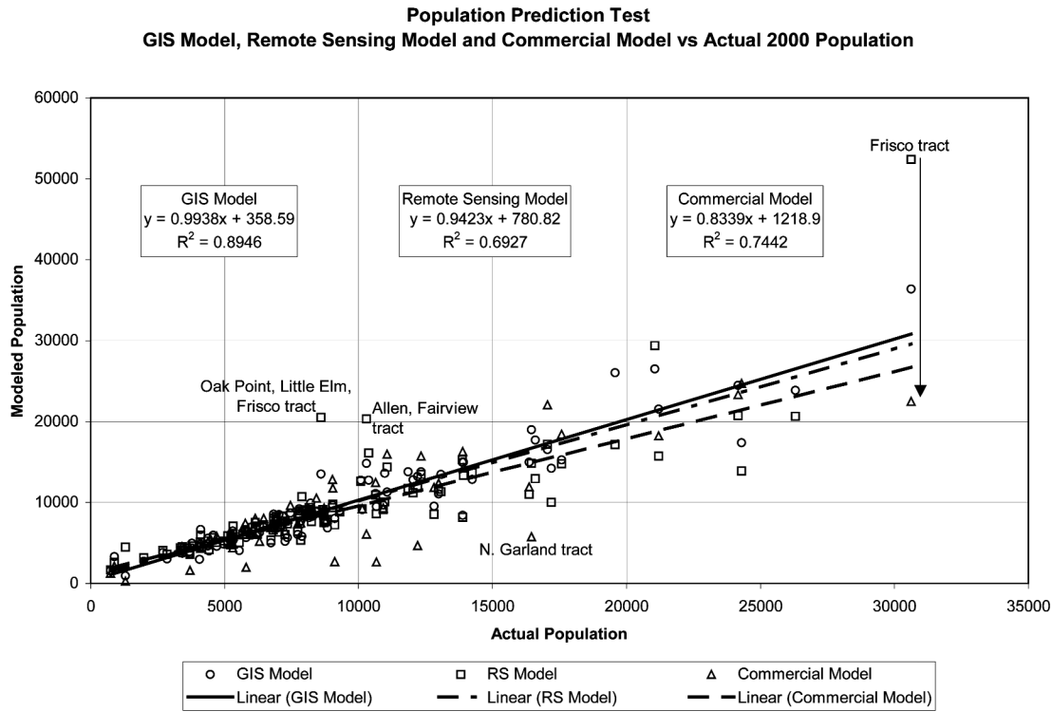

Figure 7. Cross plot of predicted population by different models and actual population in 2000 at the census tract level.

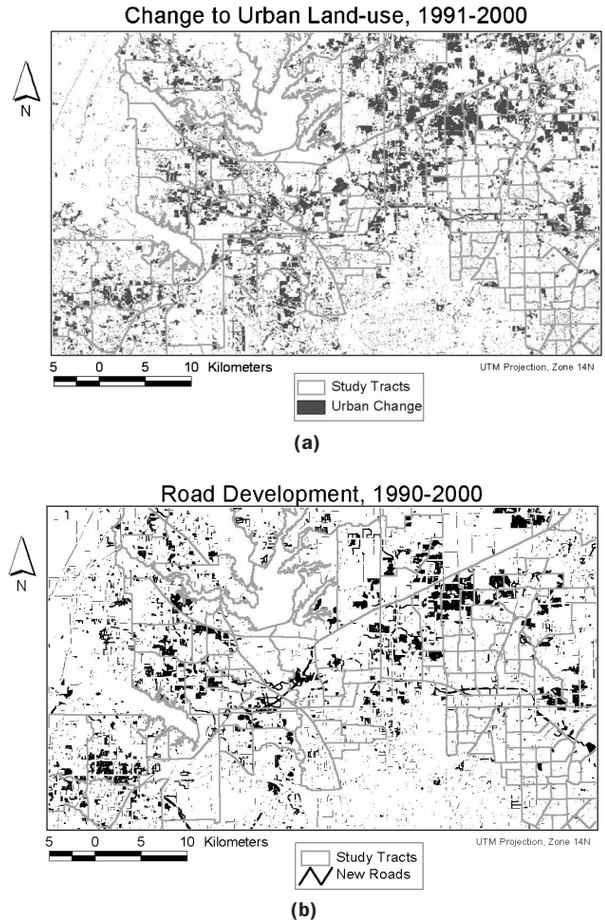

Figure 8. A zoomed view of new road and urban development (difference). (a) Urban land-use change. (b) Road development.

Conclusion

In order to obtain accurate and up-to-date population information during any intercensal years, expensive and complex demographic models are usually employed. This study explored the possibility of using remotely sensed image and GIS road network data to estimate the population growth from 1990 to 2000 in the north Dallas-Fort Worth Metroplex. The models based on remote sensing change detection and on a newly devised GIS map overlay approach were built and applied at city and census-tract levels. The population weighted average % error that normalizes the bias caused by the extreme population bases was also introduced to evaluate the accuracy of the population estimates.

The remote-sensing- and GIS-based models were found to be efficient and effective in predicting population growth at both the city and census-tract levels. At the census-tract level, the remote-sensing- and the GIS-based models yielded comparable or better accuracies when compared with a commercial demographics model. Additionally, the RS and GIS models provide direct visualization of the potential distribution of the population growth within cities and census tracts. The performance of the remote-sensing-based models, however, are spatial scale dependent. Remote-sensing-based models achieved a better accuracy at the macro level than at the micro level, similar to the conclusion drawn by Lo (1995). This can be explained by the spatial resolution of the imagery used, which determines the scale of an accurate representation of raster data. A pixel size of 30 meters or so is sufficient for land-use classification at the macro scale, but fails to provide detailed classification at the micro level with satisfactory accuracy. It is expected that the use of images acquired by recently launched high spatial resolution remote sensing satellites, such as Ikonos, could improve the accuracy of detailed image classification and improve the population model at the micro level.

Overall, the GIS-based models using new road development demonstrated the greatest potential in population estimation. They were much simpler to implement and were consistently better than the traditional remote-sensing-based and commercial demographic models. Unlike remote sensing based models, the GIS-based models were insensitive to the spatial scale and achieved robust estimates and reliable accuracies at both the city and census-tract level. This is because the TIGER data is vector data, which tends to provide the same accurate representation at all levels. It is also expected that, with the use of a more accurate GIS road network provided by commercial data vendors, the GIS-based model could accomplish an even better population estimation.

Finally, it is important to mention that the population growth models used in this study assumed a general uniform population density per unit area or per unit length of road in the study area. The cities in the study area have undergone similar suburbanization processes from 1990 to 2000. However, changes in the economy and demographic profiles could affect the ability of the model to predict population changes in the future. Recalibration of the model would be necessary in other areas with different population density in order to achieve accurate population estimaton.

References

Dobson, J.E., E.A. Bright, P.R. Coleman, R.C. Durfee, and B.A. Worley, 2000. LandScan: A global population database for estimating populations at risk, *Photogrammetric Engineering & Remote Sensing*, 66:849–857.

Epstein, J., K. Payne, and E. Kramer, 2002. Techniques for mapping urban sprawl, *Photogrammetric Engineering & Remote Sensing,* 68:913–918.

Jensen, J.R., F. Qiu, and K. Patterson, 2001. A Neural network image interpretation system to extract rural and urban land use and land cover information from remote sensor data, *GeoCarto International: A Multi-Disciplinary Journal of Remote Sensing and GIS*, 16(1):19–28.

Jensen, John R., 1996. *Introductory Digital Image Processing*, Prentice Hall, Upper Saddle River, New Jersey, 318 p.

Lo, C.P., 1986. Accuracy of population estimation from medium-scale aerial photography, *Photogrammetric Engineering & Remote Sensing*, 52:1859–1869.

———, 1995. Automated population and dwelling unit estimation from high-resolution satellite images: A GIS approach, *International Journal of Remote Sensing*, 16(1):17–34.

———, 2001. Modeling the population of China using DMSP operational Linescan system nighttime data, *Photogrammetric Engineering & Remote Sensing*, 67:1037–1047.

Longley, P.A., and V. Mesev, 2002. Measurement of density gradients and space-filling in urban systems, *Papers in Regional Science*, 81:1–28.

Lunetta, R.S., and C.D. Elvidge, 1998. *Remote Sensing Change Detection*, Ann Arbor Press, Chelsea, Michigan, 318 p.

Malila, W.A., 1980. Change vector analysis: An approach for detecting forest changes with Landsat, *Proceedings, LARS Machine Processing of Remotely Sensed Data Symposium*, 03–06 June, W. Lafayette, Indiana (Laboratory for the Applications of Remote Sensing), Purdue University, pp. 326–336.

Michalack, W.Z., 1993. GIS in land use change analysis: Integration of remotely sensed data into GIS, *Applied Geography*, 13:28–44.

Noin, D., 1970. *La Population Rurale du Maroc*, Presses Universitaires de France, Paris, France.

Ormsby, T., and J. Alvi, 1999. *Extending ArcView GIS*, Environmental Systems Research Institute, Redlands, California, 527 p.

Qiu, F., K. Woller, and R. Briggs, 2002. Prediction of population in Dallas-Forth Worth Metroplex based on road development and remote sensing change detection analysis, *Proceedings of the Association of American Geographers 98th Annual Meeting*, 19–23 March, Los Angeles, California, unpaginated CD-ROM.

Sutton, P., 1997. Modeling population density with night-time satellite imagery and GIS, *Computing, Environment and Urban Systems*, 21:227–244.

USGS, 1992. *Standards for Digital Line Graphs for Land-Use and Land Cover Technical Instructions*, Referral STO-1-2, U.S. Government Printing Office, Washington, D.C., 60 p.

Watkins, J.F., and H.A. Morrow-Jones, 1985. Small area population estimates using aerial photography, *Photogrammetric Engineering & Remote Sensing*, 51:1933–1935.

Weeks, J.R., M.S. Gadalla, T. Rashed, J. Stanforth, and A.G. Hill, 2000. Spatial variability in fertility in Menoufia, Egypt, assessed through the application of remote sensing and GIS technologies, *Environment and Planning A*, 32:695–714.

Woller, K.L., 2001. Urban Growth Detection from Remote Sensing, Master's Project, University of Texas at Dallas, Richardson, Texas, http://www.utdallas.edu/~klwoller/urban_growth/index.htm, last accessed 15 October 2002.

Yang, X., 2002. Satellite monitoring of urban spatial growth in the Atlanta metropolitan area, *Photogrammetric Engineering & Remote Sensing*, 68:725–734.

Zhan, X., C. Huang, J. Townshend, R. DeFries, M. Hansen, C. Dimiceli, R. Sohlberg, J. Hewson-Scardelletti, and A. Tompkins, 1998. Land cover change detection with change vector in the red and near- infrared reflectance space, *IGARSS '98*: *IEEE International Geoscience and Remote Sensing Symposium Proceedings*, 06–10 June, Seattle, Washington, 2:859–861.